

## NUMERICAL SIMULATION OF WATER DROPLET EVAPORATION FROM POROUS MEDIUM

Rafael Sartim, [rsartim@gmail.com](mailto:rsartim@gmail.com)

Neyval Costa Reis Jr., [neyval@gmail.com](mailto:neyval@gmail.com)

Jane Méri Santos, [janemeri@npd.ufes.br](mailto:janemeri@npd.ufes.br)

Vinicius De Martin Sarnaglia, [viniciusdms@gmail.com](mailto:viniciusdms@gmail.com)

Elisa Valentin Goulart, [elisavalentim@gmail.com](mailto:elisavalentim@gmail.com)

Universidade Federal do Espírito Santo, Centro Tecnológico, Departamento de Engenharia Ambiental, Av. Fernando Ferrari, s/n, 29060-970, Vitória, ES, Brasil

**Abstract.** *The investigation of the impingement and evaporation of droplets in porous media is a subject of great interest for several industrial applications, such as oil industry, textile, medical and inkjet printing technology. Experimental results in the literature indicate that there is a significant importance of the capillary transport of liquid during the evaporation process. Most modeling attempts for this class of problems are based on a volume average approach. However, the length scale of the problems of evaporation of droplets is comparable to the size of the pores, i.e. pore scale is around tens or hundreds of micrometers ( $10^{-4} - 10^{-5}$  m), while size of the region occupied by liquid is of the order of millimeters or tenths of millimeters ( $10^{-3} - 10^{-4}$  m). In this sense, the use of a volume averaged form of the governing equations may not represent adequately the microscopical transport phenomenon occurring. This suggests application of mathematical models that represent the mass transport in microscopical level, incorporating effect of the randomness of the porous matrix upon the transport of liquid and vapour during the phenomenon. In this work, a three-dimensional pore scale model is used to simulate the evaporation process, where the porous media is represented as a regular matrix of pores (with a randomly varying diameter) connected by a series of bonds, where the diameters of the pores and bonds vary randomly according to probability distribution functions characterizing the porous medium. In order to analyze the accuracy of the proposed model, it is compared with experimental data which represents the evaporation of 1.5 mm water droplets impinged on 400  $\mu\text{m}$  glass beads. The results show a good agreement in the distribution of liquid phase during the process of evaporation but the evaporation rate is overestimated by the simulation. This fact is explained by the existence of liquid film formed within the porous medium during the evaporation. These liquid flows are not taken into account in the numerical simulation.*

**Keywords:** *Porous media, Droplets evaporation, Pore network models*

### 1. INTRODUCTION

The experimental study and mathematical modeling of the impingement and evaporation of droplets liquid in porous media is an important subject in a wide range of practical applications, since industrial applications such as superficial treatment of materials and design of printers using inkjet printing technology (Oliver et al, 1994 and Alleborn and Raszillier, 2004), to applications in environmental problems such as use of pesticides and environmental impact studies of the release of hazardous liquid into the atmosphere (Westin et al, 1998 and Griffiths and Roberts, 1999).

For this class of applications the difficulties are usually related to complexity of mass transport and phase change inside the porous medium. After impinged droplet impact of a droplet of liquid on a porous surface, it lies in a porous medium format that resembles a semi-spheroid whose shape and dimensions depend on the balance sheet between the effects of capillarity and dissipation of momentum. The liquid fills the pores of the substrate in a small volume near the surface occupying a region of the order of several millimetres in radius and a few millimetres in depth (Reis et al, 2006). In the early stages, the evaporation occurs mainly in a region located near the interface between atmosphere and porous medium. During this period, the evaporation rate is approximately constant and depends entirely of the external parameters of the porous medium, such as velocity, vapour content and temperature of the air stream. However, evaporation causes a gradual reduction of concentration of liquid in the region near the surface, so that evaporation inside the porous medium becomes increasingly important (Figure 1). Thus, process becomes dominated by the transport mechanisms within the porous medium and less dependent on the properties of the airflow over the surface.

The complexity of the physical processes involved in this type of problems have motivated several experimental and theoretical studies, Baines & James (1994), Roberts and Griffiths (1995), Westin et al. (1998), Griffiths and Roberts (1999). One of the main challenges for development of mathematical models is determining the shape of the droplet after impingement and absorption in the porous medium and its variation along the evaporation (Roberts, 1996). Although the transport mechanisms inside a porous medium are fairly well understood, the complex interaction between the momentum of the impinging droplet, surface tension forces outside the porous medium and capillary transport inside the porous medium present serious difficulties to any modeling attempt.

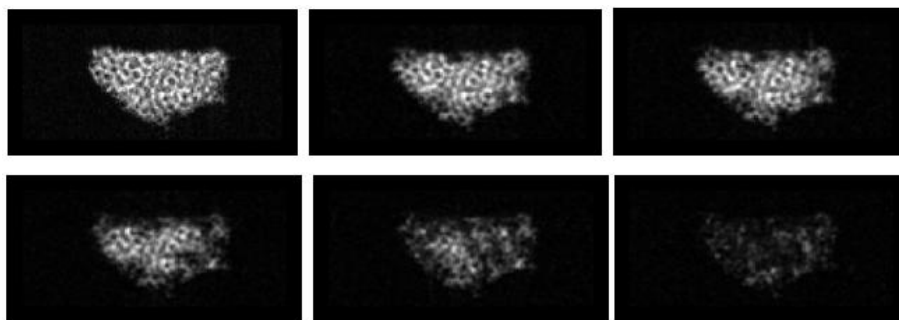


Figure 1 – Images of the shape of the water droplet inside the porous medium during drying process (REIS *et al.*, 2003).

Moreover, the redistribution of liquid due to liquid transport inside the porous medium during evaporation is often underestimated, leading to deficiency evaporation rate prediction. The evaporation models recently used for hazard assessment purposes follow two main approaches: (i) those considering the theory of a receding evaporation front, and (ii) those using the diffusion equation to predict the transport of liquid and vapor inside the porous medium. The theory of the receding evaporation front assumes that the droplet is absorbed in the porous substrate and held very near the surface. As evaporation progresses, the upper liquid front of the impinged droplet recedes in the porous substrate, whilst the base of the impinged droplet maintains its original position. Thus, vapor transport in the atmosphere is characterized by two phenomena, the molecular diffusion of vapor through the pore network from the liquid front to the surface interface, and diffusion of vapor through the interfacial layer in the atmosphere. This approach has been widely used and has proven their applicability in a wide range of practical situations, Griffiths (1991), Roberts (1996) and Griffiths and Roberts (1999).

Other authors (Westin *et al.*, 1998) argue that the main problem with this approach is that it does not consider the liquid transport inside the porous substrate, which may result in an immediate transition to a steep falling rate drying with a substantial underestimation of the evaporation rate. Westin *et al.* (1998) proposed a new approach to the problem based on the use of the diffusion equation to predict the transport of liquid and vapor inside the porous substrate. The representation of the liquid and vapor movement in the porous medium through the use of diffusion equations has been quite widespread in industrial applications, such as Nasrallah and Perre (1988). The work by Westin *et al.* (1998) is the first reported attempt to use this formulation for hazard assessment purposes.

Experimental data obtained by Reis *et al.* (2003) provided strong evidence that the approach that uses the diffusion equations is more appropriate than the one of receding front. The importance of capillary transport during evaporation causes substantial redistribution of liquid during the process. However, current approaches (Westin *et al.*, 1998) that uses the diffusion equations for vapor and liquid, are not able to incorporate such redistribution, since it considers one-dimensional approach to the problem. Moreover, the problem of droplet evaporation in porous medium has characteristics that difficulties the use of mathematical models based on the theory of a continuous medium. For a variety of situations studied by Reis *et al.* (2003), Mantle *et al.* (2003) and Reis *et al.* (2006), Nuclear Magnetic Resonance (NMR - Nuclear Magnetic Resonance) study was carried out to provide images of the shape of droplet inside the porous medium after the impingement and throughout the evaporation episode. The results show that the drying process does not advance homogeneously through the liquid region. This behavior can be mainly attributed to inhomogeneities in the porous medium. In fact, evaporation occurs along the entire boundary of the droplet, even in the deeper layers of the porous medium. Many authors (Figus *et al.*, 1999 and Yotis *et al.*, 2001) reported that the use of the hypothesis of a continuous medium and empirical transport coefficient may have considerable inadequacy, especially in conditions where the pores of the medium show a very wide diameters size distribution. Moreover, the pore scale occupied by the liquid, in the porous medium, is around  $10^{-3}$  -  $10^{-4}$  m and pores scale of the medium of interest (such as sand, for example) is around  $10^{-4}$  -  $10^{-5}$  m. Therefore, a droplet absorbed by a porous medium may have a diameter of tens or hundreds of pores, making the representation as a continuous medium clearly questionable for this class of problems.

Those factors lead to the choice of models that has better representation of the phenomena microscopic study. Prat (1993) was the first to propose the use of pore-scale models for drying simulation from porous medium, including the prediction of evaporation rates and distribution of liquid. This class of models represents mass transport at the pore scale, incorporating the microscopic features of mass transport between the pores of the medium and neglects the idea of a continuous medium. Several works have been presented in the literature using this technique to simulate the evaporation of liquids in porous medium, including the ones that faces problems involving a single fluid, Yotis *et al.* (2001), or multi-phase flow problems, Blunt (2001).

In the present work a pore-scale model is used to simulate the evaporation of a water droplet in a medium composed of 400  $\mu\text{m}$  glass beads. Such models have the potential to represent the mass transport at pore scale by incorporating the microscopic features of mass transport between the pores of the medium that improves the prediction of the capillary transport of liquid, which is one of the major challenges in the current models in literature (Reis *et al.*, 2006).

## 2. METHODOLOGY

Pore network models are based on a network representation of the porous structure. A sketch of the microstructure is shown in Fig. 2.

The main idea of this method is to describe the structure of the porous medium (Figure 2a), as a series of pores and connections (Figure 2b), ranging in diameter according to the statistical distribution characterizing its microstructure (Chandler et al, 1982). The pore bodies serve as containers for either of the two phases (liquid + vapor) with relatively large section that contains both fluids. The throats are the segments having a minimum cross-section between two pores. It is assumed that the pores do not offer resistance or capillary to the mass flow of either fluids, only acting as reservoirs. The porous medium is represented by the standard approximation of a 3-D network of spherical pore bodies connected through cylindrical throats (Figure 2c) (Prat, 1993 e Yiotis et al, 2001).

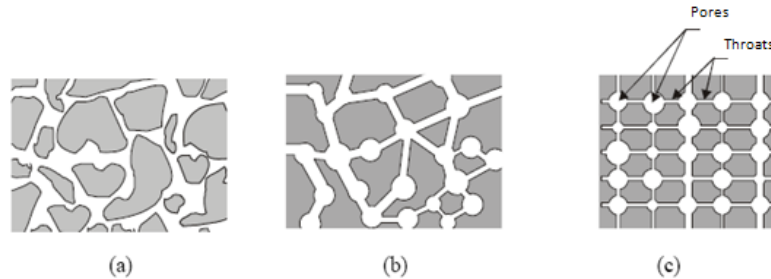


Figure 2 – Representation of the microstructure of the porous medium as a series of pores with different diameters and connections.

The throats works as conducts for fluid between the pores, when a stationary meniscus (interface) lies at the entrance of a throat adjacent to a liquid pore (Figure 3(a)), an interfacial pressure difference, calculate by Eq. (1) where  $\gamma$  is the surface tension and  $r$  the radius of the throat, develops between the two neighboring pores. The meniscus remains stationary until the pressure difference between the two pores exceeds that capillary pressure threshold. Then the meniscus Will recede instantly (Figure 3(b), (c) and (d)), since it is assumed that the throat has no volume and the gas phase penetrates the pores (Yiotis et. al., 2001).

$$P_c = \frac{2\gamma}{r} \quad (1)$$

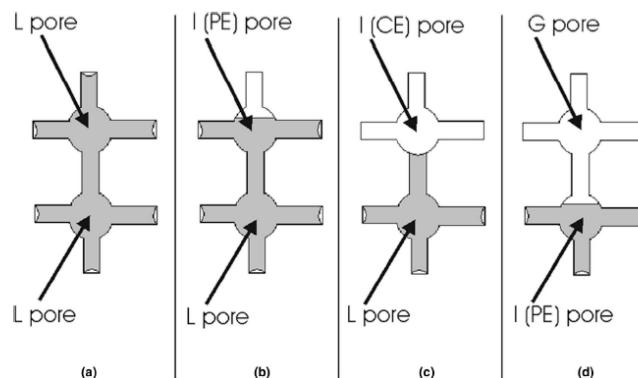


Figure 3 - The evolution of drying consisting of two liquid pores. (a) Initially the cluster is surrounded by pores completely empty of liquid. (b) When the pressure difference at the upper throat exceeds its capillary resistance, the meniscus recedes and the pore is penetrated by the gas phase. The same transition takes place between (c) and (d). (Yiotis et al., 2001)

Simulations have been carried out for  $30 \times 16 \times 30$  pore networks, where only the pores that compose the shape of the impinging droplet are saturated by liquid (water). The distance between two pores is  $2,524 \cdot 10^{-4}$  m. The throat radius are distributed randomly between and 0.15 and 0.41 percent of the medium size, which is  $400 \mu\text{m}$ , and the porous radius are distributed randomly between and 0.25 and 0.96 percent of the medium size. In general, the pore network model used in this study is the same used in Goulard et. al.( 2007).

As a result of the drying process, the liquid will reside, in general, in two different and evolving regions: a “continuous” cluster (CC), which is part of the initial liquid cluster and various “disconnected” clusters (DC), which have become disconnected from the CC and from one another (see Figure 4).

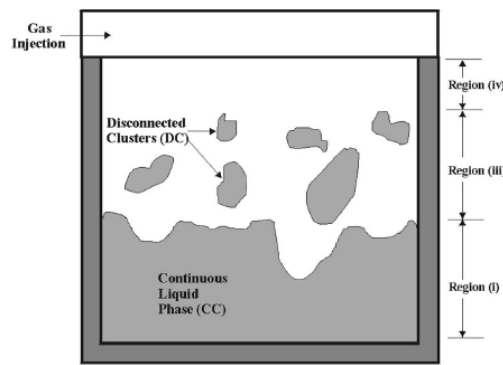


Figure 4 – Schematic representation of typical saturation patterns. (Yiotis et al., 2001).

## 2.1. Formulation

Liquid evaporates at the gas - liquid interface at rates determined by mass transfer in the gas phase, which are governed by diffusion. The evaporation rate at pores is given by

$$F_{ij} = \frac{DA_i}{L}(C_i - C_j) \quad (2)$$

where  $F_{ij}$  is the evaporation flow through a throat connecting neighboring pores  $i$  and  $j$ ,  $D$  is diffusion coefficient of the liquid component vapors in the gas phase through the porous medium,  $C_i$  is concentration at the liquid pore, which is by default equal to the equilibrium concentration  $C_e$  of the liquid component vapors and  $C_j$  is the concentration at the adjacent pore which is empty of liquid.

The phase distribution of liquid / vapor interface is located inside the pores, and depends on the mass transport in the gas phase (air + vapour). Thus, the vapor concentration inside the porous medium is calculated based on mass balance described by the equation:

$$V_i \frac{\Delta C_i}{\Delta t} = \sum_{i=1}^6 \frac{DA_i}{L}(C_i - C_j) \quad (3)$$

Where  $V_i$  is the volume of pore  $i$ ,  $\Delta C_i$  is change in  $C_i$  during the elapsed time and  $l$  is the distance between two adjacent pores  $i$  and  $j$ .

The transportation of gas from the surface to the atmosphere incorporates the theory of Brutsaert (1982) and can be handled in two parts. In the sublayer adjacent to surface transportation is performed by molecular diffusion within the Kolmogorov microscale. Above the sublayer the vertical profile of gas concentration is described by the similarity that takes into account the atmospheric stability conditions. The two parts are coupled forming a equation for the external transport that governs the flow of gas from the surface into the atmosphere. The outlet mass flow is given by

$$E_e = v_r(C_i - C_r) \quad (4)$$

Where  $v_r$  is the characteristic coefficient of the external transport and depends basically on the friction velocity of air flow (Griffiths and Roberts, 1999).,  $C_i$  is the concentration on the surface of the porous medium and  $C_r$  is the reference concentration in the atmosphere, which is considerate equal to zero.

The Figure 5 shows how the equations 2,3 and 4 are applied at the pore network matrix. The governing equation (Eq. 2) is solved in all pores occupied by gas phase subject to the following boundary conditions: (i) the concentration of  $C$  at the pore surface region occupied by liquid is considerate as the concentration of saturation vapor in the gas phase, ie, pore filled or partially empty neighbors are considered the same as the liquid saturation concentration, and (ii) flow condition prescribed on the surfaces of porous media exposed to the atmosphere, in order to simulate the removal of the vapor by the flow. The sequence of the solution algorithm is the same described in Goulard et. al. (2007).

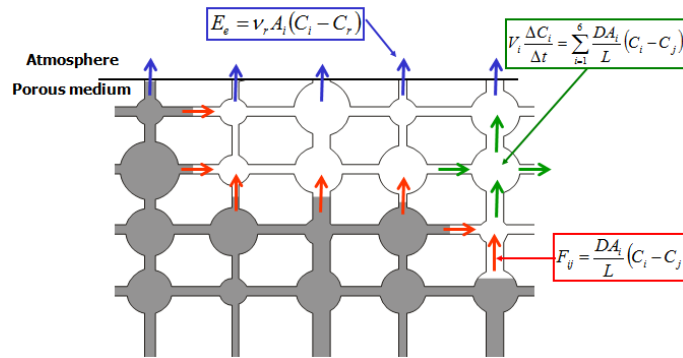


Figure 5 – Schematic representation of the mass balance inside the porous matrix.

## 2.2. Representation of the droplet and the porous medium

The porous medium is defined as a system consisting of spherical particles with diameters sufficiently small and equal, and thus can be considered a capillary model. The spherical particles can be packed bed in different ways. The pore size depends on the packed type or arrangement of spheres. The angle ( $\theta$ ) between the particles can vary in the range of  $90^\circ$  (Figure 6a) to  $60^\circ$  (Figure 6b). The first case is the less packed (cubic packed bed) and the second case the more packed (hexagonal packed bed). Aiming to represent the porous medium composed of glass beads with a diameter ( $d_p$ ) of  $400\mu\text{m}$ , we constructed a porous network with diameters ranging between  $0.485$  and  $0.127 d_p$ , considering a uniform distribution between the cubic and hexagonal packed bed (Luikov, 1966). Analogously, the diameter of the connections was considered a uniform distribution, between  $0.41 d_p$  and  $0.155 d_p$ , representing a cubic and hexagonal packed bed. Following the same criteria, geometric distance between the pores should be between  $0.577 d_p$  and  $1.0 d_p$ . For the present work, it was selected a distance between porous equal to  $0.577 d_p$  to maintain the porosity,  $\epsilon$ , of the porous medium of  $0.41$  that is similar to those determined experimentally.

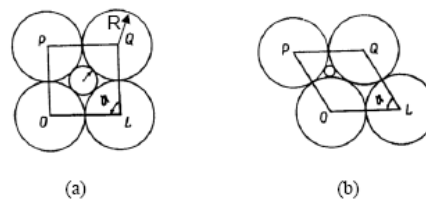


Figure 6 - Schematic representation of the geometric determination of the pore size in a packed bed of perfectly spherical particles. (a) cubic packed bed ( $\theta = 90$ ). (b) hexagonal packed bed ( $\theta = 60$ ). (Luikov, 1966)

The droplet absorbed in the porous medium has a shape of a semi-spheroid, where the aspect ratio will depend on the porous medium and the characteristics of the liquid. On the surface the droplet shape is circular, so on the XY and YZ planes the shape of the ellipse is equal. In the experiments (Reis et al. 20003) the droplet radius before falling into the surface is  $r_0$ , after the impact the axial momentum of the droplet is transformed to radial momentum, which defines the diameter and the depth of the droplet after the total absorption. Based on the average of several experiments it is possible to relate the scattering droplet based on its initial radius  $r_0$ , (before impact), the droplet radius after the absorption,  $r_{droplet}$  and the penetration  $h_{droplet}$ . This correlation is called the spreading factor,  $R^*$  and  $H^*$  is the non-dimensional penetration depth (see Figure 7).

$$R^* = \frac{r_{droplet}(t)}{r_0} \tag{5}$$

$$H^* = \frac{h_{droplet}(t)}{r_0} \tag{6}$$

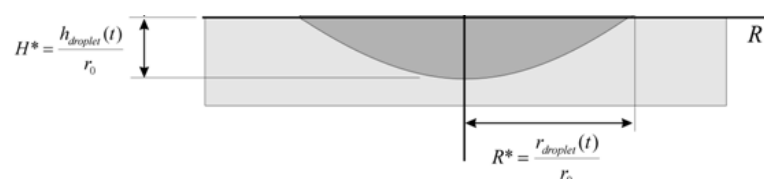


Figure 7 - Definition of the spread ratio ( $R^*$ ) and penetration depth ( $H^*$ ). (Reis 200)

The distance from the droplet to the sides of the pore network is equal to one quarter of the droplet diameter. For a 30x16x30 array, containing 14,400 pores, which only 2,119 of the pores are full of liquid at the initial time, since these form the drop. The surface of the liquid is exposed to an external air flow of 10 ml / min ( $V_r$  equal to 0007 m / s, based on atmospheric friction velocity of 0.1 m/s).

### 2.3.Parameterisation

In the initial stages of the evaporation process, all the pores in the surface are full of liquid, and the vapour concentration in the surface is equal to the saturated vapour concentration in the air. As the evaporation proceeds and the pores on the surface start to dry out, the value of the concentration of liquid in the surface,  $c_s$ , starts to be reduced and becomes dependent on the transport inside the porous medium. The value of  $c_s$  is a function of time, limiting the evaporation process. Since the value of  $c_s$  will vary from zero to the value of the saturated vapour concentration in air, it is reasonable to assume that an adequate estimate for the order of magnitude of  $c_s$  is the value of the saturated vapour concentration in air. Accordingly, a characteristic mass flux for each configuration is estimated as:

$$F_0 = v_{r0} c_{sv} \quad (7)$$

Where  $v_{r0}$  denotes the characteristic vapour transport velocity for a given flow rate and  $c_{sv}$  represents the value of the saturated vapour concentration in air. In order to determine the characteristic time scale, it is necessary to determine a characteristic area through which the flux  $F_0$  transports the mass of the liquid droplet ( $M_0$ ). A satisfactory magnitude for this area can be calculated by using the droplet radius prior to the impingement ( $r_0$ ), since the radius of the wet spot after the impingement will be larger than  $r_0$ , but of the same order of magnitude. Therefore, the time scale of the process is defined as:

$$T_0 = \frac{M_0}{F_0 A_0} \quad (8)$$

where  $A_0$  denotes the characteristic area, given as:

$$A_0 = \pi r_0^2 \quad (9)$$

This time scale represents the approximate time that an equivalent mass of liquid would take to evaporate from a fully saturated wet spot (i.e. a pool of liquid) with a radius equal to  $r_0$ , when exposed to the given air flow. The use of this time scale is important to evaluate the limiting influence of the transport inside the porous medium upon the evaporation process, and all the results presented in this work are normalised by this value. Normalising the relevant variables of the problem by using characteristic time scale,  $T_0$ , mass,  $M_0$ , and mass flux,  $F_0$ , the following dimensionless parameters were introduced:

$$T^* = \frac{t}{T_0} \quad M^* = \frac{m}{M_0} \quad F^* = \frac{F}{F_0} \quad (Dm/Dt)^* = \frac{Dm/Dt}{F_0 A_0} \quad (10)$$

Where  $T^*$  is the non-dimensional time,  $M^*$  is non-dimensional mass, also called mass fraction remaining, and  $F^*$  and  $(Dm/Dt)^*$  are the dimensionless mass flux and evaporation rate.

The concentration profiles are expressed in kg/m because they represent the integrated concentration in the horizontal plane of the impinged droplet. In the same way, it is possible to translate the actual liquid saturation concentration for the porous medium to kg/m by using the characteristic area of the impinged droplet. The characteristic area is the area of the initial wet spot determined as a function of the initial droplet radius ( $r_0$ ). It is possible to re-write the concentration of liquid as:

$$c^* = \frac{c}{c_0} \quad (11)$$

Where  $c$  is the concentration expressed in kg/m and  $c_0$  is the characteristic concentration, given as:

$$c_0 = c_{sat} A_0. \quad (12)$$

Where  $c_{sat}$  is the saturated liquid concentration ( $c_{sat} = \rho\varepsilon$ ) for the porous medium. This non-dimensional representation is very important, because it allows the characterization of the concentration profiles independently of the liquid density and the amount of liquid delivered to the porous surface.

### 3. RESULTS

The numerical results are compared with experimental results obtained by nuclear magnetic resonance (Reis et al., 2003). These techniques are images used to the 1D and 2D study. While the 2D images provide qualitative information on the drop shape after absorption and its variation during evaporation, the 1D images provided quantitatively liquid mass concentration throughout the depth of the droplet.

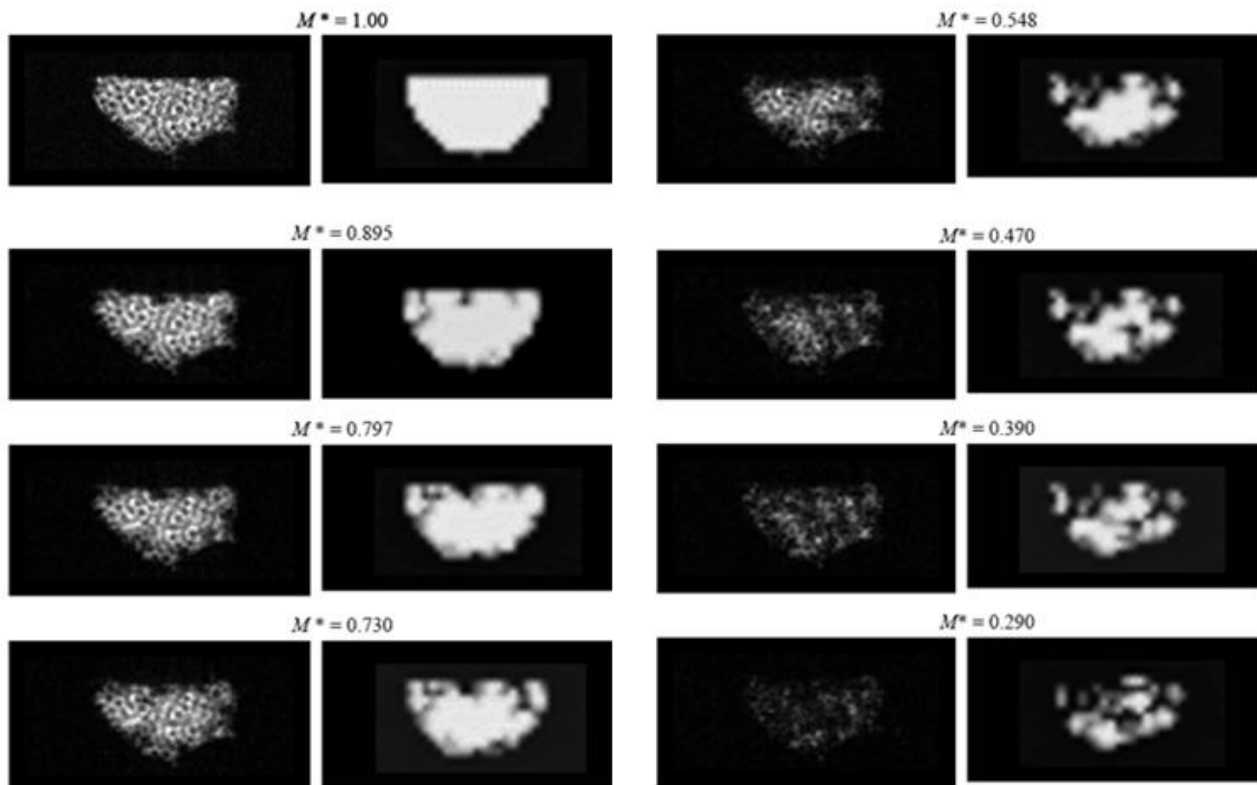


Figure 8 - Time evolution of the images of the shape of the droplet inside the porous medium. (Left side) experimental data (Reis, 2003) and (right side) numerical simulation.

Since the diameters of pores and the connections have a uniform random distribution, to represent the characteristics of random porous medium, the results presented here represent the average of several simulations. This study made an average of 9 simulations to represent the profiles concentration. The images shown here are the results of one single simulation, to allow the visibility of the effects of random characteristics of the porous medium.

Figure 8 shows the time evolution of the shape of the droplet inside the porous medium, comparing the experimental data and the simulation. Aiming to simulate the images obtained by Reis et al. (2003), the results represent the sum of the concentration in the pores of a slice of 1.5 mm drop. At the initial instant, it is possible to see a similarity in the semi-elliptical shape of the drop between the experimental and simulation results. It is important to note, the drop shape in the simulations is defined as a semi-spheroid whose dimensions represent approximately the size of the drop experiment. Each of the images shown in Figure 8 indicates a time, denoted by the level of concentration of liquid in porous medium.

It is possible to see that in the first instants of the evaporation, the surface region is losing more liquid. Over time, there is the increase of evaporation fronts significantly irregular shape, this behavior is similar to the formation of “capillary fingers”. This trend is represented adequately by the model. In the moments following the spread of fingers leads to the formation of isolated areas of liquid, both in simulation and the experimental images. For lower levels of concentration of liquid of magnetic resonance images shows liquid levels considerably lower than the simulations. This behavior is probably related to the low sensitivity of this technique to low concentrations of liquid (Reis et al., 2003 and Reis et al., 2006)

According to Reis et al (2003), the integrated concentration profiles are more suitable for displaying low levels of concentration, due to its higher sensitivity. Figure 9 shows the evolution of the concentration profile of liquid in the

vertical axis. Note that the concentration level is higher near to surface, because it is the region of greatest diameter of the droplet. By the initial concentration profiles it is possible to note that differences in initial drop shape of the experiment and the simulation generates considerable differences in concentration profiles. Notably, in the simulation results the depth of the droplet is larger than that the experiment, this happens because in the simulation the depth of the droplet was calculated based on an average of several experiments, not in an isolated experiment. Therefore, in the case of simulation the liquid is slightly more spread in the vertical direction. In the experiment, the maximum concentration is around  $c^* = 4.2$ , while the simulation does not exceed  $c^* = 3.5$ .

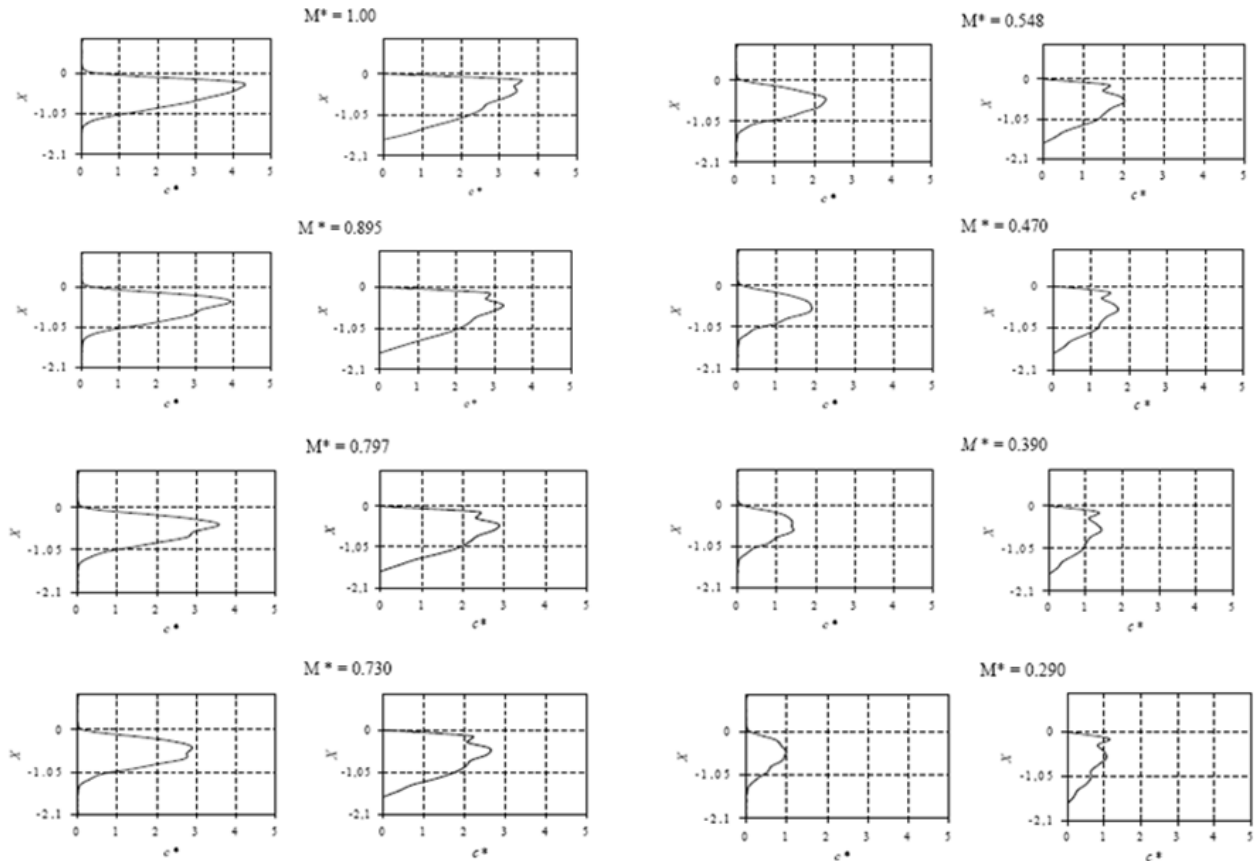


Figure 9 - Time evolution of the concentration profiles of liquid of the droplet inside the porous substrate (Left side) experimental data (Reis, 2003) and (Right side) numerical simulation.

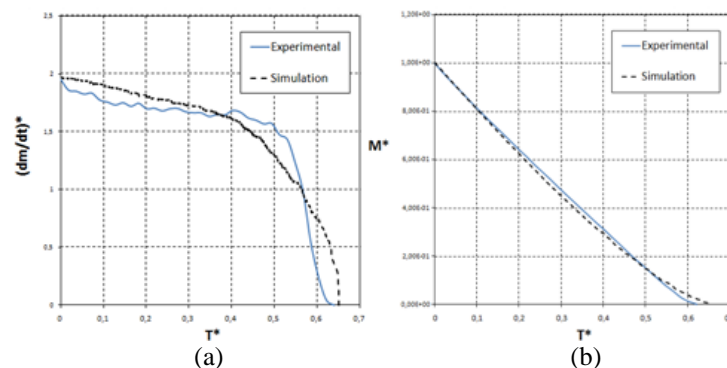


Figure 10 – (a) Non-dimensional evaporation rate  $(Dm/Dt)^*$  of the droplet vs.  $T^*$  and (b) Mass fraction of liquid remaining inside the porous medium.

As the evaporation progresses, the highest concentration is no longer in the region nearer the surface and is more in a deeper location. This phenomenon is well observed in both results, and thus the shape of the profile is changing.

The behavior of the droplet evaporation rate during the drying process is shown in Figure 10a. It is observed that during the early drying the results of the experimental data, as well as the simulation results, shows a constant evaporation rate. After a certain period the evaporation rate calculated by the simulation reduces in a shorter time



compared with the experimental. In the final moments of the process, the evaporation rate of the experiments has declined sharply while the reduction in the simulation is softer. Finally, the drying time of the simulation results is higher at around 18%. However, the general behavior of the simulation results is fairly representative. The main reason about why the process of drying is overestimated is a point that many authors (Laurindo e Prat, 1998, Yiotis et al., 2005, Prat et al. 2007) have mentioned in their studies. They have shown that this problem is attributed to the effects of liquid films developing along the connection corners between pores and that this phenomenon has a strong influence of film flows on drying rates, so the drying time is overestimated when the film effect is neglected.

Figure 10b shows the Mass fraction of liquid remaining inside the porous medium. As a consequence of the results of the evaporation rate, the behavior of the drying curve of the simulation results is in a good agreement with the experimental data. It is possible to observe that both curves (experimental and simulation) has a smooth slope throughout the process.

#### 4. CONCLUSIONS

This paper presented a scale model to simulate the pore evaporation of water droplet in a porous medium compound of 400  $\mu\text{m}$  glass beads. Aiming to assess the accuracy of the model it was compare with experimental data using images obtained by Resonance Nuclear Magnetic (Reis et al, 2003). The data used have one-dimensional profiles concentration of liquid and integrated picture of the drop of liquid absorbed by the medium porous, obtained over a time interval in which occurs the total evaporation of the liquid. Also, the evaporation rate and the mass fraction of liquid remaining inside the porous medium was taking into account.

Through comparisons, we observed that the model can predict reasonable levels of concentration of fluid in porous media during the drying process, including the formation of irregular structures similar to the formation of capillary fingers.

About the evaporation rate, the results from the numerical simulation have shown an behaviour similar to the experimental datas but the duration of the drying was overestimate. The presence of a liquid film was neglected and this seems to be the main reason of the difference from the experimental results.

#### 5. REFERENCES

- Alleborn, N., Raszillier, H., "Spreading and sorption of a droplet on a porous substrate", *Chemical Engineering Science*, 59, pp. 2071–2088, 2004.
- Baines, W. D. and James, D. F., "Evaporation of a droplet on a surface", *Ind. Eng. Chem. Res.*, vol. 33, pp. 411–416, 1994.
- Blunt, M. J., "Flow in porous media – pore-network models and multiphase flow", *Current Opinion in Colloid & Interface Science*, 6, pp. 197–207, 2001
- Brutsaert, W., "*Evaporation into the atmosphere: Theory, History and Applications*", D. Reidel, Holland, 1982
- Chandler, R., Koplik, J., Lerman, K., Willensen, J.F., "Capillary displacement and percolation in porous media.", *J Fluid Mech*, 119, pp. 249–267, 1982.
- Figus, C., Le Bray, Y., Bories, S., Prat, M., "Heat and mass transfer with phase change in a porous structure partially heated. Continuum model and pore network simulations", *Int. J. Heat Mass Transf.*, 42, pp. 2257–2569, 1999.
- Goulard, E. V., Sartim, R., Reis, N. C., Santos, J. M., 2007 "Modelagem matemática da evaporação de gotas de líquido em meios porosos através de um modelo de escala de poros", *CMNE/CILAMCE*, 2007, Porto, Portugal. *Anais do CMNE/CILAMCE* 2007.
- Griffiths, R. F., "*A model for evaporation following droplet impingement on porous surfaces*", Consultancy report to CBDE, Porton Down, UMIST, 1991
- Griffiths, R. F. and Roberts, I. D., "Droplet evaporation from porous surfaces, model validation from field and wind tunnel experiments for sand and concrete", *Atmospheric Environment*, vol. 33, pp. 3531–3549, 1999.
- Laurindo, J. B.; Prat, M. "Numerical and experimental network study of evaporation in capillary porous media. Drying rates", *Chem. Eng. Sci.*, vol.53, pp. 2257–2269, 1998.
- Luikov, A. V., "*Heat and mass transfer in capillary-porous bodies*", Pergamon Press, 1966.
- Mantle, M., Reis, N. C. Jr., Griffiths, R. F., Gladden, L. F., "MRI Studies of The Evaporation of a Single Liquid Droplet. Magnetic Resonance Imaging", v.21, n. 3-4, pp. 293–297, 2003.
- Nasrallah, S. B. and Perre, P., "Detailed study of a model of heat and mass transfer during convective drying of porous media", *Int. J. Heat Mass Transfer*, vol. 31, pp. 957–967, 1988
- Oliver, J. F., Agbezuge, L. and Woodcock, K., "A diffusion approach for modelling penetration of aqueous liquids into paper", *Colloids Surf. A: Physicochem. Eng. Aspects*, vol. 89, pp. 213–226, 1994
- Prat, M., "Percolation model of drying under isothermal conditions in porous media", *Int. J. Mult. Flow*, 19, pp. 691–704, 1993.
- Prat, M. "On the influence of pore shape, contact angle and film flows on drying of capillary porous media", *International Journal of Heat and Mass Transfer*, v. 50, p.1455–1468, 2007.

- Reis, N. C. Jr., “Droplet Impingement and Evaporation from Porous Surfaces” Ph.D. thesis submitted to the Environment Technology Centre do Department of Chemical Engineering da The University of Manchester Institute of Science and Technology, jun 2000.
- Reis, N. C. Jr., Mantle, M., Griffiths, R. F., Gladden, L. F., “Investigation of the Evaporation of Embedded Liquid droplets from porous surfaces using magnetic resonance imaging”, *International Journal of Heat and Mass Transfer*, v. 46, p.1279 -1292, 2003.
- Reis, N. C. Jr., Griffiths, R. F., Santos, J.M., “Numerical simulation of the impact of liquid droplets on porous surfaces”, *Journal of Computational Physics*, Volume 198, Issue 2, 10 August 2004, Pages 747-770, 2004.
- Reis, N. C. Jr., Mantle, M., Griffiths, R. F., Gladden, L. F., J.M. Santos “MRI investigation of the evaporation of embedded liquid droplets from porous surface under different drying regimes”, *International Journal of Heat and Mass Transfer*, v. 46, p.1279 - 1292, 2006.
- Roberts, I. D., Griffiths, R. F., “Droplet evaporation from porous surfaces; model validation from field and wind tunnel experiments for sand and concrete”, *Atmospheric Environment*, vol. 33, pp. 3531-3549, 1999.
- Roberts, I. D., “The evaporation of neat/thickened agent simulant droplets from porous surfaces”, Final report on agreement No. 2044/013/CDBE, UMIST, 1996.
- Westin, S. N., Winter, S., Karlsson, E., Hin, A. e Oeseburg, F., “On modelling of the evaporation of warfare agents on the ground”, *J. Hazardous Materials A*, vol. 63, pp. 5-24, 1998.
- Yiotis, A. G., Stubos, A. K., Boudouvis, A. G., Yortsos, Y.C., “A 2-D pore-network model of the drying of single-component liquids in porous media”, *Advances in Water Resources* 24, pp. 439-460, 2001.
- Yiotis, A. G., Stubos, I. N., Tsimpanogiannis, A. G., Yortsos, Y.C., “Pore-network modeling of isothermal drying in porous media”, *Transport Porous Media*, V. 58, pp. 63 - 86, 2005.

## 5. RESPONSIBILITY NOTICE

The authors are the only responsible for the printed material included in this paper.